Applied Mathematical Modelling 38 (2014) 1838–1845

Contents lists available at ScienceDirect

Applied Mathematical Modelling

journal homepage: www.elsevier.com/locate/apm

Computation of transmission coefficients in the plain and corrugated electro-magnetic waveguides using finite point set method

Sudhakar Matle *, S. Sundar [1]

Department of Mathematics, IIT Madras, Chennai 600036, India

ARTICLE INFO

Article history:
Received 27 August 2012
Received in revised form 9 August 2013
Accepted 25 September 2013
Available online 17 October 2013

Keywords:
Maxwell's equations
Finite point set method
Transmission coefficient
Corrugated waveguide

ABSTRACT

Maxwell's equations are solved in an electro-magnetic rectangular waveguide with the boundary determined by material properties and interface conditions wherein finite point set method approximates the partial derivatives of the scattered fields. The process is time dependent. Waveguide propagation depends on the operating wave length, polarization, shape and aspect ratio of the waveguide.

A continuous incident pulse is used to study the electric field pattern and transmission behavior in plain and corrugated waveguides. The waveguide is modeled in a 2D rectangle with incident source at the left boundary.

Transmission coefficients are computed as a function of frequency of the continuous pulse for both the plain and corrugated waveguide of various heights $\lambda/2$, $\lambda/4$ and $3\lambda/4$.

© 2013 Elsevier Inc. All rights reserved.

1. Introduction

Passive components are those that do not require electric power to operate in electrical, computer or storage systems. The study on microwave passive components like transmission lines (coaxial, rectangular and cylindrical waveguides) is essential to characterize transmission behavior and attenuation of the wave in the frequency domain. Computation of the parameters transmission coefficient and attenuation coefficient under various test defect conditions through numerical modeling and then simulation helps better understanding and proper design of microwave circuits.

As the microwave pulse incident at the source of the waveguide, the conducting walls of the waveguide control the electro-magnetic waves interior to it. The waves travel longitudinally down the waveguide till the opposite wall and then reflected back. The process results in a component of either electric field or magnetic field in the direction of propagation of the guided wave. Therefore, the wave is no longer a transverse electromagnetic wave (TEM) [1–4].

Rectangular waveguide is one of the earliest type of transmission lines [5] still commonly used in many current applications. Ratanadecho et al. [6] investigated both numerically and experimentally the heating of a liquid layer by microwave with a rectangular waveguide and showed that the heating kinetic energy depends on dielectric properties. Recently, Erol and Balik [7] introduced 2D finite difference method to analyze widely used rectangular waveguides and validated computed results with analytical solution. Tada et al. [8] employed a two dimensional finite difference time domain method in a partially filled microwave applicator to clearly describe electro-magnetic interferences and power absorption in the dielectric inserted waveguide, operating in TE_{10} mode at a frequency 2.45 GHz. Koshiba et al. [9] studied finite element analysis for electro-magnetic waveguides [10,11] in various approaches capable of suppressing and eliminating the spurious solutions.

* Corresponding author. Tel.: +91 9840269197.
E-mail addresses: iitsudha@gmail.com (S. Matle), slnt@iitm.ac.in (S. Sundar).
[1] Tel.: +91 44 22574608.

0307-904X/$ - see front matter © 2013 Elsevier Inc. All rights reserved.
http://dx.doi.org/10.1016/j.apm.2013.09.020

Nomenclature

Ω	computational domain
$x,\ y,\ z$	cartesian coordinates
t	time, s(seconds)
dx	difference between the two points ($=\lambda/20$), m(meters)
h	radius to find neighborhood points, m
λ	wave length ($=c/f$), m
f	frequency, Hz
ω	angular frequency, cycles/s
c	velocity of light ($=3\times10^8$), m/s
Nt	number of time steps
Nt_{max}	maximum number of time steps
np	total number of points
dt	magic time step, ($=\frac{dx}{2*c}$), s
f_s	sampling frequency ($=\frac{1}{dt}$), Hz
ps	picosecond
rad	radius of corrugate in *x-direction,* m
$rad1$	radius of corrugate in *y-direction,* m
$\boldsymbol{\mu}_z$	magnetic permeability, henrys/m
ϵ_z	electrical permittivity, farads/m
μ_r	relative permeability, dimensionless
$\boldsymbol{\epsilon}_r$	relative permittivity, dimensionless
σ	electrical conductivity, siemens/m
ξ_m	equivalent magnetic loss, ohms/m
E_z	electric field in z-direction, volts/m
$H_x,\ H_y$	magnetic field in x-, y-direction, amperes/m

Electro-magnetic guided waves and ultrasonic guided waves propagation through corrugation [12], bends and defects have been studied by many researchers to understand reflection and transmission characteristics at the probes. Demma et al. [13] explained the frequency dependent transmission behavior in terms of modes propagating in the straight and curved sections of the pipe using finite element method. Takahashi et al. [14] investigated a high power, 170 GHz, long pulse RF experiments of ITER relevant transmission line consisting of 63.5 mm circular corrugated waveguides [15] and successfully obtained transmission efficiency 92% from the inlet of the transmission line to the end.

Smoothed particle methods in electro-magnetic wave applications have been studied extensively. Recently, Ala et al. [16] employed pairwise interaction dynamically to solve Maxwell's equations with perfectly matched layer boundary conditions in a general 2D domain. Frequency of excitation used here is 1.8 GHz.

The present paper addresses finite point set solution [17] of Maxwell's equations in a rectangular waveguide with and without corrugation. The actual problem, governing equations and the corresponding boundary conditions are described schematically in Section 2. The developed numerical scheme wherein time derivatives discretization by central finite difference scheme while spatial derivatives approximation by finite point set method are presented systematically in Section 3. Finally, scattering of electric field results and evaluation of transmission coefficients are thoroughly discussed in Section 4.

2. Mathematical model

In order to demonstrate transmission across the waveguide, a hollow rectangular cavity is modeled in a 2D computational domain (Ω). Due to biaxial symmetry of the cavity about the two axes, only one quarter of the cross section of the cavity is considered for the present study. A lossless media is chosen to avoid electric and magnetic field losses inside the waveguide.

Fig. 1 shows the two dimensional corrugated waveguide with the excitation source $E_z->1.0*cos(k\omega dt)$, $k=1,2\ldots,Nt_{max},\ \omega=2\pi f$ at $x=0$. The corrugated plane of the waveguide is divided into two parts: corrugated space and free space. The corrugated space is rectangle in shape, have centers denoted as A (icenter,jcenter) and B (icenter,jcenter1).

A microwave beam of light passes through a waveguide, it generates electric and magnetic fields inside it. In general, microwaves are electro-magnetic waves classified by frequencies.

2.1. Governing equations

The equations which govern the electric and magnetic fields propagation that vary with time in the 2D computational domain indicated by physical laws are the Maxwell's equations. The electric field E and the magnetic field H are vector fields

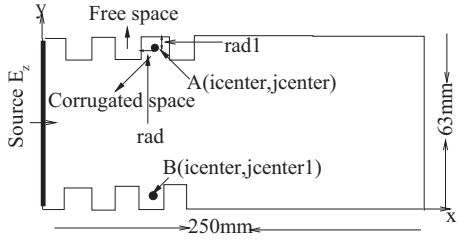

Fig. 1. A schematic computational domain for the corrugated waveguide.

have amplitudes and directions varying with three spatial coordinates $x,\ y$ and z and a time coordinate t. The waveguide is infinite along z-direction and that incident fields do not vary along z. The following assumptions are made in 2D case:

$$E_x = 0, \quad E_y = 0, \quad H_z = 0 \quad \text{and} \quad \frac{\partial}{\partial z} = 0. \tag{1}$$

Maxwell's equations in an electro-magnetic waveguide is as follows:

$$\frac{\partial H}{\partial t} = -\frac{1}{\mu}\nabla \times E \quad \epsilon\frac{\partial E}{\partial t} + \sigma E = \nabla \times H. \tag{2}$$

In cartesian form, Eq. (1) as follows:

$$\begin{aligned}
&\frac{\partial H_x}{\partial t} = -\frac{1}{\mu}\frac{\partial E_z}{\partial y} \\
&\frac{\partial H_y}{\partial t} = \frac{1}{\mu}\frac{\partial E_z}{\partial x} \\
&\frac{\partial E_z}{\partial t} = \frac{1}{\epsilon}\left(\frac{\partial H_y}{\partial x} - \frac{\partial H_x}{\partial y} - \sigma E_z\right),
\end{aligned} \tag{3}$$

where $\mu,\ \epsilon$ and σ are magnetic permeability, electric permittivity, and electrical conductivity respectively.

2.2. Boundary conditions

An incident plane wave continuous sinusoidal pulse takes into account scattered fields at the source. For the two dimensional case, a typical wave source condition at $x = 0$ (the left boundary of the cavity) is:

$$E_z = 1.0 * (cos(Nt\omega dt)) \quad Nt = 1, \ldots, Nt_{max}, \tag{4}$$

where ω is the angular frequency, Nt is the number of time steps, Nt_{max} is the maximum number of time steps and $dt = \frac{dx}{2c}$ is the magic time step. The perfect electric conductor condition, i.e., tangential component of electric field E_z is zero, employed at the remaining three boundaries.

3. Numerical scheme

Finite point set method with Lagrangian approach is used here to solve Maxwel equations numerically. The computational domain is filled with points or particles that carry microwave properties like velocity, density, electric field and magnetic field and those are moving with the wave.

Also, points distribution need not be uniform. An arbitrary point $\bar{x}$ in the computational domain is chosen for study. Point cloud of smoothing radius is constructed around $\bar{x}$ so that the points inside the cloud should neither be on the same line nor be on the same circle.

Before implementing finite point set method, time derivatives in the left hand side of Eq. (3) are discretized using central finite difference scheme. Thus, Eq. (3) simplifies as follows:

$$\begin{aligned}
&H_x|^{n+1/2} - H_x|^{n-1/2} = -\frac{\Delta t}{\mu_z}\frac{\partial E_z}{\partial y} \\
&H_y|^{n+1/2} - H_y|^{n-1/2} = \frac{\Delta t}{\mu_z}\frac{\partial E_z}{\partial x} \\
&E_z|^{n+1/2} - E_z|^{n-1/2} = \frac{\Delta t}{2\epsilon_z}\left(\frac{\partial H_y}{\partial x} - \frac{\partial H_x}{\partial y}\right).
\end{aligned} \tag{5}$$

Three fields $H_x : \Omega - > R, \quad H_y : \Omega - > R$ and $E_z : \Omega - > R$ are defined at the point $x_i,\ i = 1, 2, \ldots, np$ as:

$$H_x|_i = H_x(x_i, y_i, z_i),\ H_y|_i = H_y(x_i, y_i, z_i),\ E_z|_i = E_z(x_i, y_i, z_i) \tag{6}$$

Denote $f|_i = [H_x|_i, H_y|_i, E_z|_i]$ be the unknown function defined at points $x_i, i = 1, 2, \ldots, np$. Correspondingly, $f^0|_i = [H_x^0|_i, H_y^0|_i, E_z^0|_i]$ be the initial guess. The function f and its spatial derivatives around the point $\bar{x}$ are evaluated from the values of the same at the neighboring points using Taylor series expansion.

The spatial derivatives of the fields $E_z,\ H_x$ and H_y at a particle position $\bar{x}$ are approximated based on values of functions of its neighboring particles. A sliced Gaussian weight function with compact support h of the form:

$$\begin{aligned} w =& w(\bar{x}_i - \bar{x}; h) = exp\left(-\alpha \frac{||\bar{x}_i - \bar{x}||^2}{h^2}\right) \quad \text{if} \quad \frac{||\bar{x}_i - \bar{x}||}{h} \leqslant 1 \\ =& 0 \quad \text{elsewhere} \end{aligned} \tag{7}$$

is used to restrict number of neighboring points. The positive constant α signifies the exponential decay with a typical value $\alpha = 6$.

The set of m neighboring points around the point $\bar{x}$ inside the support of size h is denoted as $P(\bar{x}, h) = \{x_i, i = 1, 2 \ldots, m\}$. Also, $m >= 9$ and $x_i, i = 1, 2, \ldots, m$ should neither be on the same line and nor be on the same circle for consistent solution. In contrast to condition consistency, solution error increases abnormally as the number of neighboring points exceed 6 due to discontinuity at corners of the rectangular waveguide. Therefore, radius of the neighborhood h around the point $\bar{x}$ is taken as six times the space step dx.

Substituting spatial derivative approximations obtained from Taylor series expansion in (5), the resultant equation is as follows:

$$\begin{aligned} H_x|^{n+1/2} - H_x|^{n-1/2} &= -\delta b \left[\frac{\tilde{E_z}^{n+1/2} + \tilde{E_z}^{n-1/2}}{2dy_i}\right] + e_{1i}, \\ H_y|^{n+1/2} - H_y|^{n-1/2} &= \delta b \left[\frac{\tilde{E_z}^{n+1/2} + \tilde{E_z}^{n-1/2}}{2dx_i}\right] + e_{2i}, \\ E_z|^{n+1/2} - E_z|^{n-1/2} &= cb \left[\frac{\tilde{H_y}|^{n+1/2} + \tilde{H_y}^{n-1/2}}{2dx_i} - \frac{\tilde{H_x}|^{n+1/2} + \tilde{H_x}^{n-1/2}}{2dy_i}\right] + e_{3i}, \end{aligned} \tag{8}$$

where $\delta b = \frac{\Delta t}{\mu_z}, \quad cb = \frac{\Delta t}{2\epsilon_z}, \quad dx_i = x - x_i, \quad dy_i = y - y_i \quad \tilde{E_z} = E_z|_i - E_z(\bar{x}) \quad \tilde{H_x} = H_x|_i - H_x(\bar{x})$ and $\tilde{H_y} = H_y|_i - H_y(\bar{x})$.

In corrugated space, the coefficients δb and cb are defined as follows:

$$\begin{aligned} \delta b_i &= \frac{dt}{\mu_z \mu_{ri}\left(1 + \frac{dt\xi_m}{\mu_z \mu_{ri}}\right)} \\ \delta c_i &= \frac{dt}{\epsilon_z \epsilon_{ri}\left(1 + \frac{dt\sigma}{2\epsilon_z \epsilon_{ri}}\right)}, \quad i = 1, 2, \ldots, np, \end{aligned} \tag{9}$$

where np represents the total number of points.

The least square solution minimizes the error $\bar{e} = (e_{1i}, e_{2i}, e_{3i})\prime$ in the resulting system:

$$\bar{e} = M\bar{a} - \bar{b}, \tag{10}$$

where M is the matrix having entries as $\{dx_i, dy_i, dx_i^2/2, dx_i dy_i, dy_i^2/2\},\ i = 1, 2, \ldots m,\ \bar{a}$ is having entries as $\left\{\frac{\partial f}{\partial x}, \frac{\partial f}{\partial y}, \frac{\partial^2 f}{\partial x^2}, \frac{\partial^2 f}{\partial x \partial y}, \frac{\partial^2 f}{\partial y^2}\right\},\ f = H_x,\ H_y,\ E_z$ and $\bar{b}$ is a column vector having entries as $\{f|_i\}, i = 1, 2, \ldots, m$. The finite point set approximation for first order spatial derivatives are obtained from the first two rows of a 5 by 1 column vector $(M^t W M)^{-1} M^t W b$. The solution $f = H_x,\ H_y,\ E_z$ is updated over each time step dt until it reaches Nt_{max} or steady state.

4. Results and discussion

In the present section, results on electric field E_z propagation along z-direction for both the plain and corrugated waveguides, transmission behavior near the opposite boundary in a waveguide and important salient features are thoroughly discussed.

4.1. E_z propagation in plane waveguide

Numerical simulation is valid only if the space step dx and neighborhood radius h must be properly balanced for various values of frequency. Also, magic time step (dt) and the space step dx are related with a non-dimensional number $\frac{cdt}{dx} = 1/2 (< 1)$ to insure numerical stability of the method.

Electric field pattern E_z along z-direction in a plane waveguide is investigated at the three frequencies of excitation 28 GHz, 82.3 GHz and 170 GHz. Fig. 2 shows electric field E_z propagation along z-direction at $T = 400$ for 28 GHz frequency

Fig. 2. A pseudo plot of electric field (E_z) propagation in a plain waveguide at the excitation frequency 28 GHz when the time step $T = 400$.

of excitation. The blue strip represents negative values of E_z while the red[2] strip signifies positive values of E_z. At the thick red strip, E_z values are very high while they are very low at the thick blue strip. It is noticed that irregularity in electric field pattern at the corners is slowly developed once the plain wave hits the opposite boundary. The time step recorded when it hits opposite boundary is $T = 320$. Solution is unbounded for a bounded time ($320 < T < 450$) indicates numerical instability due to perfect electric conductor boundaries.

Transmission pattern of E_z along z-direction is investigated at three point locations I (0,0.0162), A (0.0324,0.0162)(middle) and C (0.08046,0.0162) (near the probe) in a plain waveguide of aspect ratio approximately 2.5 for 28 GHz frequency of excitation and shown in Fig. 3. It is observed that signal (almost one full wave in the middle and a half wave near the probe) becomes distorted at the 450th time step and after which solution is no longer stable and not suitable for study due to reflections and irregular scattering.

4.2. E_z propagation in a corrugated waveguide

A non-dimensional wavelength $\lambda_1 (= \frac{\lambda}{dx})$, icenter$(= \lambda_1 * i,\ i = 1, 2, \ldots 100)$, jcenter$(= \frac{1}{2})$, jcenter1 $(= je/2)$, rad$(= \frac{\lambda_1}{i}$, $i = 4/3, 2, 3, 4)$ and rad1$(= \frac{\lambda_1}{i}, i = 4/3, 2, 3, 4)$ are defined before numerical simulation of the corrugated waveguide.

Fig. 4 shows pseudo-plots of electric field E_z along z-direction in a corrugated waveguide of corrugation height $\lambda/2$ for frequencies of excitation 28 GHz, 82.3 GHz and 170 GHz. From the plot, it is observed that E_z scatters irregularly with the frequency.

Absolute values of E_z greater than 1 started at corners of the source boundary and propagate very quickly as soon as the wave hits the boundary opposite to the source boundary. However, propagation error rate much faster in 28 GHz excitation frequency when compared with the other two.

4.3. Evaluation of transmission coefficients

In the present problem, transmission coefficient is computed from the ratio of average over absolute FFT (fast Fourier transform) of the signal at probe points on a line probe near the boundary opposite to the source boundary to the average over absolute FFT of the corresponding incident signal points on a line source.

Transmission coefficients are computed at five specified points on the line proximity to the boundary opposite to the incident plane source and denoted as Tc1, Tc2, Tc3, Tc4 and Tc5. The coordinates of the selected five points are $(ie - 1, 1)$, $(ie - 1, je - 1)$, $(ie - 1, je/2)$, $(ie - 1, je/3)$ and $(ie - 1, 2je/3)$. The values ie and je represent the number of points in x- and y-directions respectively. It is assumed that transmission coefficient Tc_{final} at the line proximity to the boundary opposite to the source is the average over all coefficients at five points on the same line.

Fig. 5 shows the transmission coefficient (Tc) against frequency (range $= \frac{f_s}{2} * (0 : 1/300 : 1)$) in a corrugated waveguide of height $\lambda/4$ for various frequencies 28 GHz, 82.3 GHz and 170 GHz. From the plot, it clears that 'Tc' values are more than 1 in between 275 GHz to 285 GHz for the excitation frequencies 82.3 GHz and 170 GHz. It indicates solution is unbounded in that range for a bounded source and constant parameters. Therefore, it is not advisable to compute transmission lines in the frequency domain for frequencies of excitation 82.3 GHz and 170 GHz.

Fig. 6 shows transmission coefficients in the frequency domain at the probe near the proximity of the opposite boundary for both plain waveguide and corrugated waveguide of various corrugation heights $\lambda/4, lambda/2$ and $3\lambda/4$. Transmission analysis is done for frequencies ranging from 260 GHz to 300 GHz. From the plot, it clears that 'Tc' values are distributed normally over the range and variances increase with the corrugation heights. In case of plain waveguide, 'Tc' values are distributed uniformly in a straight line.

Another important fact is that transmission efficiency is 100% in the frequency range 275GHZ to 285GHZ in case of corrugated waveguide of corrugation height $\lambda/4$.

[2] For interpretation of color in Fig. 2, the reader is referred to the web version of this article.

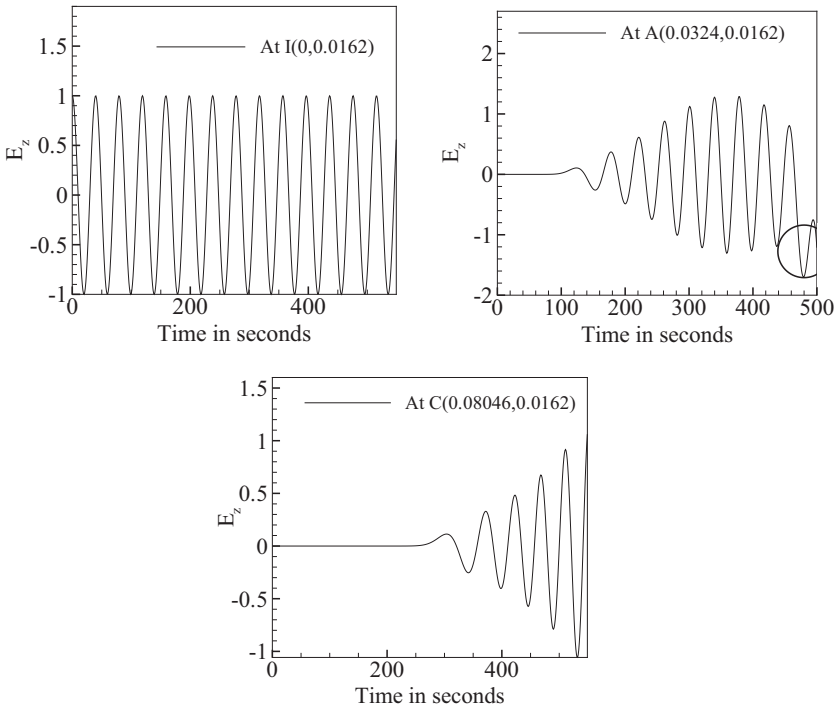

Fig. 3. Electric field E_z values along z-direction in a plain waveguide.

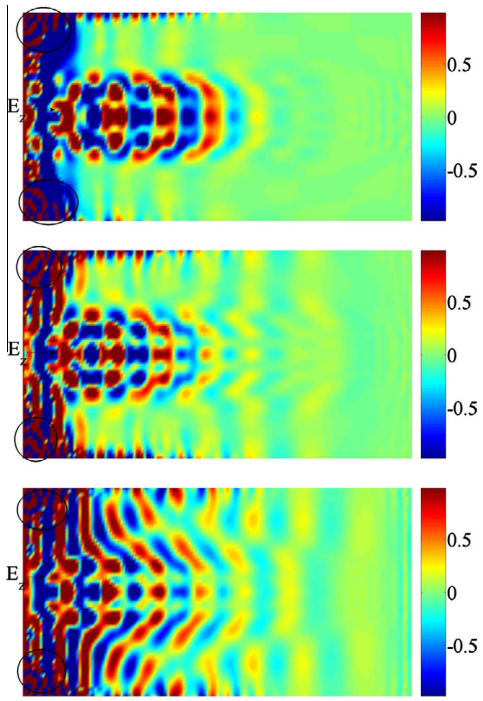

Fig. 4. E_z propagation along z-direction in a corrugated waveguide when the frequencies of excitation 28 GHz, 82.3 GHz and 170 GHz.

4.4. E_z propagation in a waveguide of aspect ratio less than 1

Electric and magnetic field patterns that exist depends on the dimension of the rectangular waveguide. Fig. 7 shows the pseudo plot of E_z propagation along z-direction in a waveguide of the aspect ratio 0.6 for 28 GHz frequency of excitation. From the plot, it clears that stability of the solution is achieved to certain extent with the current aspect ratio <1.

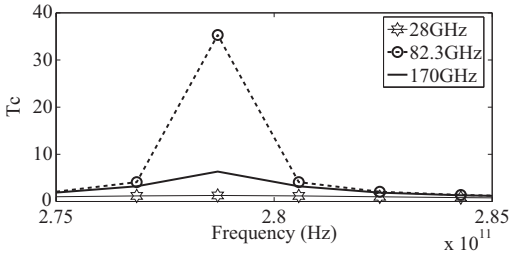

Fig. 5. Transmission coefficients at the proximity of the opposite boundary for a corrugated waveguide of height $\lambda/4$ for various frequencies 28 GHz, 82.3 GHz and 170 GHz.

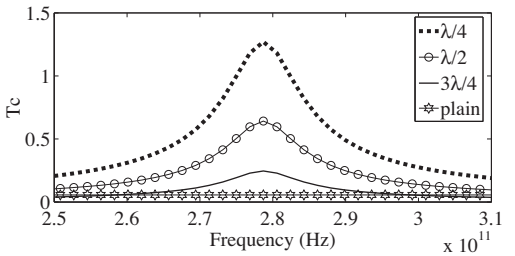

Fig. 6. Transmission coefficients at the proximity of the opposite boundary for a plain waveguide and corrugated waveguide of various corrugation heights $\lambda/4$, $\lambda/2$ and $3\lambda/4$.

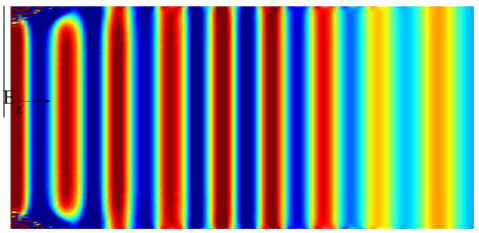

Fig. 7. Pseudo plot of electric field E_z propagation along z-direction at the time step $T = 400$ for a plain waveguide of the aspect ratio 0.6.

5. Conclusions

In view of results and discussions, the following conclusions are drawn.

- As the frequency increases from 28 GHz to 170 GHz, transmission loss also increases in a plane waveguide.
- Computed transmission coefficients have been plotted against frequency and concluded that transmission efficiency decreases with an increase of the corrugation height.
- Finite point set method produced better results in terms of efficiency and stability when compared to the finite element method and the finite difference method at the higher frequency of excitation. FDM, a 5-point set mesh less method, required more number of time steps (approximately 100 times used in FPM) and precision color bar axis around $[-10^{-}30, 10^{-}30]$ at 28 GHz frequency of excitation. On the other hand, amount of memory and computational cost were very high for a finite element method. Also, handling of FEM mesh at corrugated grooves were very difficult in case of the corrugated waveguide.
- Aspect ratio of computational transmission line must be less than 1 to reduce solution instability and to improve transmission efficiency.

Acknowledgment

The corresponding author is very thankful to Board of Research in Fusion Science and Technology group working under National Fusion Program includes Prof. V. Subramani and B.K. Shukla for their constant discussions in developing the code finite point set method.

References

[1] A. Taflove, S.C. Hagness (Eds.), Computational electrodynamics finite difference method, 2005.
[2] E.C. Jordan, K.G. Balmain (Eds.), Electromagnetic waves and radiating systems, 2005.
[3] C.W. Hicks (Ed.), Experimental and electromagnetic modeling of the waveguide based spatial power combining systems, 2002.
[4] C.A. Balanis (Ed.), Advanced engineering electromagnetics, 2012.
[5] V.A. Bakshi, A.V. Bakshi (Eds.), Transmission lines and waveguides, 2009.
[6] P. Ratanadecho, K. Aoki, M. Akahori, A numerical and experimental investigation of the modeling of microwave heating for liquid layers using a rectagular waveguide (effects of natural convection and dielectric properties), Appl. Math. Model. 26 (2002) 449–472.
[7] Y. Erol, H.H. Balik, A new approach to analysis of rectangular waveguides, J. Sci. Technol. 2 (2) (2008) 177–193.
[8] S. Tada, R. Echigo, H. Yoshida, Numerical analysis of electromagnetic wave in a partially loaded microwave applicator, Int. J. Heat Mass Transfer 41 (4–5) (1998) 709–718.
[9] M. Koshiba, K. Hayata, M. Suzuki, Finite element method analysis of microwave and optical waveguide trends in countermeasures to spurious solutions, Electron. Commun. Jpn. (Part-2-Electron.) 70 (9) (2007) 96–108.
[10] J.H. Whealton, A 3D analysis of Maxwel's equations for cavities of arbitrary shape, J. Comput. Phys. 75 (1988) 168–189.
[11] J.P. Berenger, A perfectly matched layer for the absorption of elctromagnetic waves, J. Comput. Phys. 114 (1994) 185–200.
[12] E.J. Kowalski, D.S. Tax, M.A. Shapiro, J.R. Sirigiri, R.J. Temkin, T.S. Bigelow, D.A. Rasmussen, Linearly polarized modes of a corrugated metallic waveguide, IEEE Trans. Microwave Theory Appl. 58 (2010) 2772–2780.
[13] A. Demma, P. Cawley, M. Lowe, B. Pavlakovic, The effect of bends on the propagation of guided waves in pipes, J. Pressure Vessel Technol. 127 (3) (2005) 328–335.
[14] K. Takahashi, K. Kajiwara, A. Kasugal, N. Kobayashi, B. Pavlakovic, Investigation of Transmission Characteristic in Corrugated Waveguide Transmission Lines for Fusion Application, IEEE, 2007 (1-4244-0633).
[15] J.L. Doane, Design of circular corrugated waveguides to transmit millimeter waves at ITER, Fusion Sci. Technol. 53 (1) (2008) 159–173.
[16] G. Ala, E. Francomano, A. Tortorici, E. Toscano, F. Viola, Smoothed Particle Electromagnetics: a mesh free solver for transients, J. Comput. Appl. Math. 191 (2) (2006) 194–205.
[17] J.J. Monaghan, Simulating free surface flows with SPH, J. Comput. Phys. 110 (2) (1994) 399–406.